DOE/METC/C-96/7214

A Reduced Mechanism for Low-Heating-Value Gas Combustion in a Perfectly Stirred Reactor

Authors:
David Marlow
Thomas S. Norton

Conference Title:
American Flame Research Committee 1995 International Symposium

Conference Location:
Monterey, California

Conference Dates:
October 15-18, 1995

Conference Sponsor:
International Flame Research Foundation

DISCLAIMER

A REDUCED MECHANISM FOR LOW-HEATING-VALUE GAS COMBUSTION IN A PERFECTLY STIRRED REACTOR

D. Marlow* and T. S. Norton
Department of Energy
Morgantown Energy Technology Center
Morgantown, WV 26505

We have begun an effort to accurately model NO_x formation from the combustion of coal-derived fuels in turbine combustors. Both turbulent mixing and the chemical kinetics of ammonia oxidation are expected to have important influences upon NO_x formation rates. This paper concentrates upon the development of a model for the kinetics. Previous empirical, kinetic mechanisms have inaccurately assumed equilibrium OH concentrations and ignored the chemistry of HCN, an important intermediate. We have developed a reduced mechanism by applying simplifying assumptions to a full, detailed mechanism for methane combustion with nitrogen chemistry. The mechanism contains 7 rates for 10 non-steady-state species, a single partial equilibrium assumption, and steady-state relations for 18 species. The Zeldovich and Fenimore mechanisms of NO formation are modeled, as is the NO recycle mechanism by which NO is converted to HCN. Nitric oxide formation from N_2O is also included. Two oxidation routes for NH_3 are included: the first describes NH_3 conversion to N, and then to NO; the second describes HNO formation, and final conversion of HNO to NO. Stirred reactor calculations were performed for three cases: (1) methane-air combustion with no nitrogenated species in the reactants, (2) methane-air combustion with 1000 ppmV NO in the reactants, and (3) methane-air combustion with 1000 ppmV NH_3 in the reactants. The reactor temperature (1300 to 2000 K) and residence time (10^{-4} to 10^{-1} s) were varied. Both the reduced and skeletal mechanism calculations agree very well with calculations using the detailed mechanism of Miller and Bowman, except for fuel-rich combustion at low temperatures (less than 1500 K), where results from the skeletal mechanism begin to deviate due to neglect of C_2 chemistry. Future work will test the performance of the reduced and skeletal mechanisms in models of laminar, counterflow flames, which are meant to represent flamelet combustion in a turbulent flame.

I. Introduction

Our goal is to properly model the production of NO_x from NH_3 during the combustion of low-heating-value gas in industrially relevant flames. We are most interested in the flames in turbine combustors as implemented in coal-gas-fueled combined cycle systems. These flames are premixed or mostly premixed, pressurized, and turbulent.

Turbulent flame modelers frequently neglect the chemical kinetics of fuel conversion because the fuel consumption reactions occur in thin spatial regions, rapidly converting the reactants to their equilibrium state. Ammonia in the fuel is also consumed rapidly in thin spatial regions; however, ammonia is typically not converted to its equilibrium products. The fractions of NO, N_2, and HCN formed depend strongly upon kinetics. Relative production rates of these species vary

*NRC Resident Research Associate

greatly with varying equivalence ratio, flame residence time, temperature, and hydrocarbon concentration in the fuel. Since NH_3 oxidation is sensitive to the kinetics and the kinetics is in turn sensitive to the flame environment, a kinetic mechanism should be incorporated to accurately model NO_x formation in turbulent flames.

A simple, empirical kinetic mechanism for NH_3 conversion has been included previously in a model of a turbulent, jet flame (Drake et al., 1984). The mechanism contains two global reactions to form NO and N_2. Formation of HCN is not considered. The global rates are written as the products of Arrhenius coefficients, the NH_3 concentration, and the equilibrium OH concentration. The jet is modeled for a low turbulent Reynolds number and varying NH_3 concentration. Predictions and measurements for the jet show similar trends with varying NH_3 concentration, but the predicted NO_x emissions are consistently 50% greater than measured.

Several assumptions made by Drake et al. probably limit both the accuracy and range of applicability of their empirical mechanism. First, neglect of HCN chemistry should cause inaccuracies for all but lean, premixed combustion, since HCN is frequently important as both an intermediate and a product of NH_3 conversion for fuel-rich conditions. Hydrogen cyanide is especially important as a product of rich-stage combustion in a two-stage reactor since the HCN created in the first stage is converted to NO in the second stage. Second, though the equilibrium OH concentration has been applied in the rate calculations, we cannot expect to be able to correlate NH_3 conversion with an equilibrium OH concentration over the entire flame. Instantaneous data from laser-based experiments (Barlow and Carter, 1994) indicate that the region of a jet flame near its tip is nearly equilibrated at the state defined by the instantaneous mixture fraction. However, near the nozzle flamelet-like behaviour occurs, resulting in OH concentrations far from equilibrium. More detailed descriptions of both the nitrogen and hydrocarbon oxidation kinetics are needed, especially to accurately model the influence of non-equilibrium radical concentrations on NO_x conversion.

Though rates and minor pathways may still be controversial, the detailed kinetic mechanism for low-heating-value gas combustion is well understood at atmospheric pressure. However, due to computational limitations the full mechanism cannot be used for industrially relevant flames. Peters (1991) has developed a method for reducing the detailed mechanism. First, reactions are eliminated from the full, detailed mechanism to create the minimum possible reaction set (called a skeletal mechanism) capable of accurately modeling the system of interest. Then partial-equilibrium and steady-state assumptions are applied to create algebraic expressions for short-lived intermediates, and global reactions are formulated for the remaining non-steady state species. Because reduced mechanisms are simplifications of detailed mechanisms, they provide computationally tractable models that are more closely representative of the full chemistry than empirical, global rates.

Several researchers are actively developing reduced mechanisms for NO_x formation. Chung and Lee (1993) have modeled laminar, counterflow diffusion flames of natural gas. Only the

Zeldovich mechanism for NO formation is considered in their calculations. Glarborg et al. (1992) have considered methane combustion in a perfectly-stirred reactor. The Glarborg reduced mechanism includes the Fenimore and Zeldovich pathways, HCN oxidation, and the NO recycle mechanism to reduce NO to HCN. Lindstedt and Selim (1994) have accurately modeled NH_3 oxidation in premixed flames of hydrogen and air. The allowed pathways to NO_x formation are NH_3 destruction and the Zeldovich mechanism. Of these efforts, the work by Glarborg et al. comes closest to incorporating all of the reactions necessary to model low-heating-value gas combustion. However, we cannot directly apply the Glarborg mechanism because NH_3 oxidation is not included. The Lindstedt mechanism does include NH_3 oxidation, but does not include carbon-containing species. Current mechanisms must be extended or combined.

We have adapted the work of Lindstedt and Glarborg to create a "combined" reduced mechanism for low-heating-value gas combustion. Our skeletal mechanism contains all the reactions of the Glarborg skeletal mechanism, with 20 reactions added to this set to model NH_3 chemistry. Glarborg's steady-state equations are rederived to account for the added reactions, and three new steady-state equations are introduced for three species added to the system by the new reactions. The resulting reduced mechanism has 7 reaction rates for 10 non-steady state species and 18 steady-state and partial-equilibrium equations.

The model is tested for a wide range of conditions in a perfectly stirred reactor (PSR). The PSR is chosen as a well-defined representation of the distributed reaction zones observed in turbulent flames. Future work will consider another environment characteristic of turbulent flames, namely, flamelet combustion.

The next section defines the skeletal mechanism. Following this the reduced mechanism is derived. Then the mechanism is validated against skeletal and detailed calculations for a wide range of conditions in the PSR.

II.   Skeletal Mechanism

The skeletal mechanism is shown in Table I. The first 77 reactions in the table are taken directly from Glarborg et al. (1992) The rates of these reactions are based on a full detailed mechanism of Glarborg (unpublished), which is an update of the mechanism published by Miller and Bowman. The remaining 20 reactions of Table I are added based on the work of Lindstedt and Selim, with rate coefficients from Miller and Bowman. Figures 1 through 6 contain curves calculated with: (1) the reduced mechanism derived in the next section, (2) the skeletal mechanism of Table I, and (3) the detailed mechanism of Miller and Bowman, with the rate for the reaction, $CH + N_2 = HCN + N$, taken from the more recent measurements of Dean et al. (1990). The mechanism of Miller and Bowman is used for comparison in this study because of its ready availability and general acceptance.

3

The greatest difference between the detailed mechanism and the skeletal mechanism is the neglect of the chemistry of C_2 and higher hydrocarbons in the skeletal mechanism. The C_2 chemistry has a secondary effect on NO_x kinetics through the formation of soot and soot precursors, which lower the temperature and decrease NO_x formation through the thermally sensitive Zeldovich mechanism. The only direct effect of C_2 chemistry on NO_x kinetics occurs through the reaction, $\cdot HCCO + NO = HCNO + CO$, which is an important path to reduce NO to HCN and N_2 at low-temperature, fuel-rich conditions. The reactions associated with NO_2 formation and destruction in the skeletal mechanism are also neglected since NO_2 emissions are insignificant in this study.

For low-heating-value gas combustion at typical operating conditions, most of the NO_x formation results from NH_3 oxidation. The chief path for NH_3 conversion is through the nitrogen atom. Ammonia is converted to N by reaction with H, O, and OH. The resulting N then participates in the reactions of the extended Zeldovich mechanism. In the absence of ammonia, N is chiefly produced through the rate-limiting Zeldovich reaction:
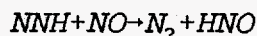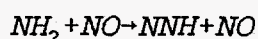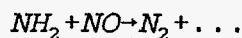
$$N_2 + O = N + NO$$
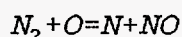
Another less important but generally significant path from NH_3 to NO is through HNO:

$$NH_3 \rightarrow NH_2 \rightarrow HNO \rightarrow NO$$
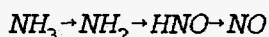
Again, this path occurs by reactions with O, H, and OH.

Ammonia can also play a very important role in reducing NO through the paths:

$$NH_2 + NO \rightarrow N_2 + \ldots$$
$$NH_2 + NO \rightarrow NNH + NO$$
$$NNH + NO \rightarrow N_2 + HNO$$

The remaining HNO is also reduced to molecular nitrogen through the path,

$$HNO \rightarrow NH \rightarrow N \rightarrow N_2$$

All of these paths are brought about by reactions with O, H, OH, and N-species. No hydrocarbon species (in fact, no carbon containing species) participates in any of the reaction pathways discussed thus far.

When hydrocarbons are present, another important route to NO production and destruction occurs

through HCN. Production of NO occurs via the Fenimore mechanism chiefly by the pathway:

$$CH + N_2 \rightarrow HCN \rightarrow NCO \rightarrow NH \rightarrow N \rightarrow NO$$
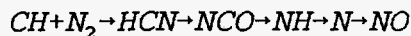
In the absence of oxygen, the HCN is not oxidized to NO, but remains as a stable product. For more fuel rich situations, recycle of NO to HCN and N_2 becomes important:

$$NO + CH \rightarrow HCN \rightarrow N_2$$
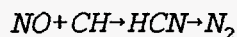
This pathway causes the reduction of NO observed in reburning.

Our domain of interest also includes low-temperature, fuel-lean combustion. Under these conditions, the N_2O mechanism for NO formation becomes significant:

$$N_2 + O + M \rightarrow N_2O \rightarrow NO$$
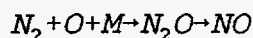
III. Reduced Mechanism

The skeletal mechanism is reduced to seven rate equations by applying partial equilibrium and steady state assumptions. Application of the steady-state assumption here assumes that the change in concentration from a species' initial value is small relative to the rates of production and destruction. The assumption leads to an algebraic expression for the concentration of the steady-state species. Since there are no derivatives in the conservation equations for the PSR, the equations for all species are algebraic equations, and little or no reduction in computational effort results from the steady-state assumptions. When convection and diffusion are important to a problem, finite differencing is applied. Then the steady-state assumption decouples the species equations for each node, resulting in significant simplifications to the numerical problem.

The following species are assumed in steady state: O, CH_3, $^3CH_2$, $^1CH_2$, CH_2OH, CH_2O, CH, HCO, C, HO_2, CN, NCO, NH, N, N_2O, NH_2, NNH, HNO. The first 15 of these were assumed in steady-state by Glarborg et al. (1992). The last three species are added here for NH_3 conversion. In addition, OH is assumed in partial equilibrium. The steady-state assumptions for the first 15 species listed above have been tested thoroughly for combustion in a PSR by Glarborg et al. (1992), as has the partial equilibrium assumption for OH. The validity of the steady-state assumptions for the 3 remaining species (NH_2, NNH, HNO) has been established in low-pressure, premixed flames by Lindstedt et al. The validity of these assumptions for PSR conditions is established by the agreement between the skeletal and reduced mechanisms observed

5

below.

Many of the steady-state equations derived originally by Glarborg et al. remain unchanged by our additions to the skeletal mechanism. However, they will be repeated here to avoid propagating errors. The partial equilibrium relation for OH is:

$$[OH] = \frac{k_{b3}[H_2O][H]}{k_{f3}[H_2]}$$

The steady-state assumptions are:

$$[O] = \frac{\sqrt{B^2 - 4AC} - B}{2A}$$

where,

$$A = k_{f16}(N_O + k_{f11}[CH_4])$$

$$B = N_O N_{CH_3} - k_{f16}(\omega_{f1} + \omega_{b2} + \omega_{f4} - \omega_{f10} - \omega_{f12})$$

$$C = N_{CH_3}(\omega_{f1} + \omega_{b2} + \omega_{f4})$$

$$N_{CH_3} = k_{b10}[H_2] + k_{b12}[H_2O] + k_{f13}[H] + (k_{b18} + k_{b19})[OH]$$

$$N_O = k_{b1}[OH] + k_{f2}[H_2] + k_{b4}[H_2O] + k_{f11}[CH_4]$$

$$[CH_3] = \frac{\omega_{f10} + \omega_{f11} + \omega_{f12}}{k_{b10}[H_2] + k_{b12}[H_2O] + k_{f13}[H] + k_{f16}[O] + (k_{b18} + k_{b19})[OH]}$$

6

$$[^3CH_2] = \frac{\omega_{f14} + \omega_{f17} + S_{39}(\omega_{b15} + \omega_{b18})}{N._{^3CH_2} - S_{39}k_{b39}[M]}$$

$$S_{39} = \frac{k_{f39}[M]}{N._{^1CH_2}}$$

$$N._{^1CH_2} = k_{f15}[H_2] + k_{f18}[H_2O] + k_{f39}[M] + k_{f40}[O_2] + k_{f41}[CO_2]$$

$$N._{^3CH_2} = k_{b14}[H_2] + k_{b17}[H_2O] + (k_{f31}[M] + k_{f32})[H]$$
$$+ (k_{f33} + k_{f34})[NO] + (k_{f35} + k_{f36})[OH]$$
$$+ (k_{f37} + k_{f38})[O_2] + k_{b39}[M]$$

$$[^1CH_2] = \frac{\omega_{b15} + \omega_{b18} + \omega_{b39}}{N._{^1CH_2}}$$

$$[CH_2OH] = \frac{\omega_{b19} + \omega_{f20}}{k_{f19}[H] + k_{f23}[M] + k_{f24}[O_2]}$$

$$[CH_2O] = \frac{\omega_{f16} + \omega_{f23} + \omega_{f24} + \omega_{f35} + \omega_{f37} + \omega_{f41} + \omega_{f47}}{k_{f25}[H] + k_{f26}[OH]}$$

$$[CH] = \frac{\omega_{f32} + \omega_{f36}}{N_{CH} - (S_{42} + S_{45})(k_{f42}[H] + k_{f45}[OH])}$$

7

$$N_{CH} = k_{b32}[H_2] + k_{b36}[H_2O] + k_{f42}[H] + k_{f43}[NO] + (k_{f44} + k_{f45})[OH]$$
$$+ k_{f46}[O_2] + k_{f47}[H_2O] + k_{f48}[CO_2]$$

$$S_{42} = \frac{k_{b42}[H_2]}{N_C}$$

$$[C] = \frac{\omega_{f42} + \omega_{f45}}{N_C}$$

$$S_{45} = \frac{k_{b45}[H_2O]}{N_C}$$

$$N_C = k_{b42}[H_2] + k_{b45}[H_2O] + k_{f49}[OH] + k_{f50}[O_2]$$

$$[HCO] = \frac{\omega_{f25} + \omega_{f26}}{k_{f22}[CH_3] + k_{f27}[M] + k_{f28}[H] + k_{f29}[OH] + k_{f30}[O_2]}$$

$$[HO_2] = \frac{\omega_{f6} + \omega_{f24} + \omega_{f30}}{k_{f7}[H] + k_{f8}[OH] + k_{f21}[CH_3]}$$

$$[CN] = \frac{\omega_{f62} + \omega_{f70} + \omega_{f74}}{k_{b62}[H_2O] + k_{f64}[OH] + k_{f65}[O_2]}$$

$$[NCO] = \frac{\omega_{f60} + \omega_{f63} + \omega_{f64} + \omega_{f65}}{k_{f66}[H] + k_{f67}[OH] + k_{f68}[NO]}$$

8

$$[NH] = \frac{U_{NH} - S_{54B} k_{f54}[NO]}{N_{NH}}$$

$$N_{NH} = k_{f51}[H] + (k_{f52} + k_{f53} + k_{f54})[NO] + k_{b82}[H_2]$$
$$+ k_{b83}[H_2O] + (k_{b84} + k_{f86} + k_{f87})[OH] + (k_{f88} + k_{f97})[O_2]$$

$$U_{NH} = \omega_{b51} + \omega_{b52} + \omega_{b53} + \omega_{f61} + \omega_{f66} + \omega_{f81}$$
$$+ \omega_{f82} + \omega_{f83} + \omega_{b86} + \omega_{b87} + \omega_{b88} + \omega_{b97} + S_{54B}(\omega_{b58} + \omega_{f68})$$

$$S_{54B} = \frac{k_{b54}[H]}{k_{f58}[M] + (k_{b54} + k_{f59})[H]}$$

$$[N] = \frac{U_N}{N_N}$$

$$N_N = (k_{b53} + k_{f55})[OH] + k_{b51}[H_2] + k_{f56}[O_2] + k_{f57}[NO]$$
$$+ k_{f76}[CO_2] + k_{f77}[CH_3] + k_{b86}[H_2O]$$

$$U_N = \omega_{f51} + \omega_{f53} + \omega_{b55} + \omega_{b56} + \omega_{b57} + \omega_{f69} + \omega_{f70} + \omega_{f75} + \omega_{f86}$$

$$[NH_2] = \frac{U_{NH_2}}{N_{NH_2}}$$

$$U_{NH_2} = \omega_{f78} + \omega_{f79} + \omega_{f80} + \omega_{b81} + \omega_{b82} + \omega_{b83}$$
$$+ \omega_{b84} + \omega_{b85} + \omega_{b90} + \omega_{b92} + \omega_{b96}$$

$$N_{NH_2} = k_{f81}[H] + k_{b78}[H_2] + k_{b79}[H_2O] + (k_{b80} + k_{f82})[OH]$$
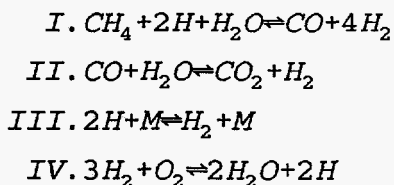$$+ (k_{f83} + k_{f84})[NO] + (k_{f85} + k_{f92})[NO] + k_{f90}[NNH] + k_{f96}[HNO]$$

$$[N_2O] = \frac{\omega_{f54} + \omega_{b58} + \omega_{f68} + \omega_{b59}}{k_{f58}[M] + (k_{b54} + k_{f59})[H]}$$

$$[NNH] = \frac{\omega_{b89} + \omega_{b90} + \omega_{b91} + \omega_{f92}}{k_{f90}[NH_2] + k_{f91}[NO] + (k_{f89} + k_{b92})[OH]}$$

$$[HNO] = \frac{\omega_{f84} + \omega_{f87} + \omega_{f91} + \omega_{b93} + \omega_{b94} + \omega_{b95} + \omega_{b96} + \omega_{f97}}{k_{b91}[N_2] + k_{f93}[M] + (k_{b84} + k_{b87} + k_{f94})[H] + k_{f95}[OH] + k_{b97}[NO] + k_{f96}[NH_2]}$$

where ω_{fi} is the forward reaction rate of reaction number i. Since the nitrogen chemistry is not expected to significantly alter combustion, none of the reactions describing the nitrogen chemistry appears in steady-state equations for non-nitrogen containing species.

The four reactions of the reduced mechanism that describe combustion are taken from Glarborg et al. (1992); our derivation is identical to theirs, but we will repeat the reactions and rates here for completeness and to avoid propagating errors. Glarborg et al. developed the rates following the well-established procedure of Peters and coworkers, adding net production rates of steady-state species to eliminate elementary rates from the reduced rate. Glarborg et al. also truncated several of the global rates, neglecting the less significant elementary reactions in the summations. The reduced reactions are:

$$I. \quad CH_4 + 2H + H_2O \rightleftharpoons CO + 4H_2$$
$$II. \quad CO + H_2O \rightleftharpoons CO_2 + H_2$$
$$III. \quad 2H + M \rightleftharpoons H_2 + M$$
$$IV. \quad 3H_2 + O_2 \rightleftharpoons 2H_2O + 2H$$

The rates for these equations are:

10

$$\omega_I = \omega_{10} + \omega_{11} + \omega_{12} - \omega_{13} - \omega_{22}$$

$$\omega_{II} = \omega_9$$

$$\omega_{III} = \omega_5 + \omega_6 + \omega_{13} + \omega_{19} - \omega_{20} - \omega_{21} + \omega_{22} + \omega_{24} + \omega_{28} + \omega_{29} + \omega_{30}$$

$$\omega_{IV} = \omega_1 + \omega_7 + \omega_{20} + \omega_{21} + \omega_{37}$$

where ω_i represents the difference of the forward and reverse rates for reaction i.

Normally, in the course of developing a reduced mechanism, we would now formulate global rates for the nitrogen chemistry. For instance we could express NO formation as $N_2 + O_2 = 2NO$. Of course this expression has no physical meaning since N_2 does not react directly with O_2. The main purpose of this equation is to handle bookeeping for production and destruction of the species in the different reactions. But, because NO only appears in a single global reaction, and N_2 and O_2 concentrations are nearly unaffected by the rate of NO formation, global rates for the nitrogen chemistry are unnecessary. Instead, we can express the net rates of production of the nitrogenated species directly. Again adding rates of steady-state species to eliminate elementary reactions, we have arrived at the following reduced expressions for the net rates of production of the nitrogenated species:

$$\omega_{NO} = -2\omega_{54} - 2\omega_{57} + \omega_{61} + \omega_{66} + \omega_{67} - \omega_{68} + \omega_{69} + \omega_{70} - \omega_{71} - \omega_{72} - \omega_{73}$$
$$- \omega_{74} - \omega_{77} + \omega_{81} + \omega_{82} + \omega_{83} + \omega_{84} - \omega_{85} - \omega_{92}$$

$$\omega_{HCN} = -\omega_{61} - \omega_{66} - \omega_{67} - \omega_{68} + \omega_{69} + \omega_{70} + \omega_{71} + \omega_{72} + \omega_{73} + \omega_{74} + \omega_{77}$$

$$\omega_{NH_3} = -\omega_{81} - \omega_{82} - \omega_{83} - \omega_{84} - \omega_{85} - \omega_{89} - \omega_{90} - \omega_{91}$$

IV. Reduced Mechanism Validation

The stirred reactor was modeled using the PSR FORTRAN program written at Sandia, with CHEMKIN II and the Sandia database for transport and thermochemistry. Minor modifications were made to allow modeling with reduced mechanisms.

Figures 1, 2 and 3 show the performance of the mechanism over a range of reactor residence

times for a constant reactor temperature of 1700 K. The smallest time, $\tau = 10^{-4}$ s, represents the approximate residence time in a flame front, while the largest time, $\tau = 10^{-1}$ s, is about the residence time in a turbine combustor. Three cases were considered: (1) methane-air combustion with no nitrogenated species in the reactants (Fig. 1), (2) methane-air combustion with 1000 ppmV NO in the reactants (Fig. 2), and (3) methane-air combustion with 1000 ppmV NH_3 in the reactants (Fig. 3). The first two cases are identical to those considered by Glarborg et al. (1992) and are only reproduced here to show that no accuracy has been lost in expanding the mechanism. The third case is meant to represent syn gas combustion with a typical NH_3 level from a gasifier.

The agreement is generally very good for all cases and mechanisms considered. The excellent agreement observed between the reduced and skeletal mechanisms for all conditions suggests that the steady-state and partial-equilibrium assumptions applied to create the reduced mechanism are sound. The largest discrepancies observed are those for the detailed and skeletal mechanisms at fuel-rich conditions where C_2 chemistry and reactions between nitrogenated species become more important. A small part of the discrepancy is caused by small changes in the elementary rate coefficients which were previously introduced by Glarborg. As Fig. 3 suggests, no major NH_3 pathway appears to have been neglected. Nor do any of the added reactions affect the agreement observed by Glarborg et al. (Figs. 1 and 2).

Figures 4, 5, and 6 show tests of the same three cases for varying reactor temperature (1300 K to 2000 K) at a fixed residence time of 10^{-2} s. The agreement is generally the same as that observed in Figs. 1, 2, and 3, with the largest discrepancy observed for fuel-rich, low-temperature combustion. Again, most of the discrepancy observed arises from the neglect of C_2 chemistry in the skeletal mechanism.

V. Summary

A reduced mechanism has been created to model syn-gas combustion with NH_3 present in the reactants. The mechanism contains rates for 10 non-steady-state species (CH_4, H_2, O_2, CO, H_2O, H, CO_2, N_2, NO, HCN, and NH_3), as well as a partial equilibrium relation for one species (OH), and steady-state relations for 18 species (O, CH_3, $^3CH_2$, $^1CH_2$, CH_2OH, CH_2O, CH, HCO, C, HO_2, CN, NCO, NH, N, N_2O, NH_2, NNH, HNO). The reduced mechanism is based on a skeletal mechanism containing 96 reactions which were chosen to model hydrocarbon oxidation and nitrogen chemistry with an emphasis on correct prediction of radical concentrations.

All performance calculations were executed for a perfectly stirred reactor. Three cases were considered: (1) methane-air combustion with no nitrogenated species in the reactants, (2) methane-air combustion with 1000 ppmV NO in the reactants, and (3) methane-air combustion with 1000 ppmV NH_3 in the reactants. Both the reduced and skeletal mechanism calculations agree very well with calculations using a detailed mechanism for a range of reactor residence

times (10^{-4} to 10^{-1} s, T = 1700 K) and temperatures (1300 to 2000 K, $\tau = 10^{-2}$ s). The largest discrepancies were observed for fuel-rich combustion at low temperatures. For these conditions, the skeletal mechanism disagrees with the detailed mechanism, suggesting that C_2 reactions important for these conditions have been neglected in the skeletal mechanism.

Future work will test the performance of the reduced and skeletal mechanisms in models of laminar, counterflow flames. If the mechanisms succeed in modeling the chemistry in both the PSR and these flames, then we expect them to succeed in modeling turbulent flames, which are composed primarily of distributed reaction zones (similar to combustion in the PSR) and flamelets (similar to counterflow flames).

Acknowledgements

References

Barlow, R. S. and Carter, C. D. (1994): *Combust. Flame*, 97:261-280.

Chung, S. H. and Lee, S. R. (1993): in Reduced Kinetic Mechanisms for Applications in Combustion Systems (Peters and Rogg, Eds.), Lecture Notes in Physics m15, Springer-Verlag, p. 308.

Dean, A. J., Davidson, D. F., Hanson, R. K., and Bowman, C. T. (1990): *Twenty-third Symposium (International) on Combustion*, The Combustion Institute, p. 259.

Drake, M. C., Pitz, R. W., Correa, S. M., and Lapp, M. (1984): *Twentieth Symposium (International) on Combustion*, The Combustion Institute, p. 1983.

Glarborg, P., Kee, R. J., Grcar, M. D., and Miller, J. A. (1986): PSR: A Fortran Program for Modeling Well-Stirred Reactors, Sandia Report SAND86-8209, Sandia National Laboratories, Livermore, CA.

Glarborg, P., Lilleheie, N. I., Byggstoyl, S., Magnussen, B. F., Kilpinen, P., and Hupa, M. (1992): *Twenty-fourth Symposium (International) on Combustion*, The Combustion Institute, p. 889.

Kee, R. J., Rupley, F. M., and Miller, J. A. (1989): CHEMKIN-II: A Fortran Chemical Kinetics Package for the Analysis of Gas-Phase Chemical Kinetics, Sandia Report SAND89-8009, Sandia National Laboratories, Livermore, CA.

Lindstedt, R. P. and Selim, M. A. (1994): *Combust. Sci. and Tech.*, 99:277-298.

Miller, J. A. and Bowman, C. T. (1989): *Prog. Energy Combust. Sci.*, 15:287-338.

Peters, N. (1991): in Reduced Kinetic Mechanisms and Asymptotic Approximations for Methane-Air Flames (Smooke, Ed.), Lecture Notes in Physics 384, Springer-Verlag, p. 48.

Table I: Skeletal mechanism for methane/air combustion with NH_3 present in the reactants. Units are cal, moles, cm, and s. Rates for the first 77 reactions are taken from Glarborg et al. (1992), while the rates for the last 20 reactions are from Miller and Bowman.

		A	β	E
1.	$H+O_2 <=> O+OH$	3.5E+16	-0.70	17070
2.	$O+H_2 <=> OH+H$	5.0E+04	2.67	6290
3.	$OH+H_2 <=> H_2O+H$	5.9E+08	1.37	3520
4.	$OH+OH <=> H_2O+O$	2.1E+08	1.40	-400
5.	$H+OH+M => H_2O+M$	7.5E+21	-2.00	0
	Third Body Efficiencies: N_2/2/ CO_2/4/ H_2O/15/			
6.	$H+O_2+M => HO_2+M$	7.0E+17	-0.80	0
	Third Body Efficiencies: H_2O/18.6/ CO_2/4.2/ H_2/3.33/ CO/2.11/			
7.	$HO_2+H => OH+OH$	2.5E+14	0.00	1900
8.	$HO_2+OH => H_2O+O_2$	3.9E+13	0.00	-50
9.	$CO+OH <=> CO_2+H$	1.5E+07	1.30	-760
10.	$CH_4+H <=> CH_3+H_2$	2.2E+04	3.00	8750
11.	$CH_4+O => CH_3+OH$	3.7E+07	1.91	7690
12.	$CH_4+OH <=> CH_3+H_2O$	1.3E+06	2.18	2530
13.	$CH_3+H => CH_4$	2.6E+28	-5.11	-2627
14.	$CH_3+H <=> {}^3CH_2+H_2$	9.0E+13	0.00	15100
15.	${}^1CH_2+H_2 <=> CH_3+H$	5.8E+13	0.00	0
16.	$CH_3+O => CH_2O+H$	8.4E+13	0.00	0

17.	$CH_3+OH <=> {}^3CH_2+H_2O$	3.8E+06	2.00	5000
18.	${}^1CH_2+H_2O <=> CH_3+OH$	7.5E+15	-1.00	0
19.	$CH_2OH+H <=> CH_3+OH$	1.0E+14	0.00	0
20.	$CH_3+O_2 => CH_2OH+O$	1.3E+13	0.00	26900
21.	$CH_3+HO_2 => CH_2OH+OH$	2.0E+13	0.00	0
22.	$CH_3+HCO => CH_4+CO$	3.0E+13	0.00	0
23.	$CH_2OH+M => CH_2O+H+M$	1.1E+43	-8.00	43000
24.	$CH_2OH+O_2 => CH_2O+HO_2$	1.5E+13	0.00	690
25.	$CH_2O+H => HCO+H_2$	2.2E+08	1.77	3000
26.	$CH_2O+OH => HCO+H_2O$	3.4E+09	1.18	-447
27.	$HCO+M => H+CO+M$	1.9E+17	-1.0	17020
Third Body Efficiencies: CH_4/2.8/ CO/1.9/ CO_2/3.0/ H_2/1.9/ H_2O/5.0/				
28.	$HCO+H => CO+H_2$	7.2E+13	0	0
29.	$HCO+OH => CO+H_2O$	1.1E+14	0	0
30.	$HCO+O_2 => CO+HO_2$	7.6E+12	0	400
31.	${}^3CH_2+H+M => CH_3+M$	2.4E+31	-4.38	0
32.	${}^3CH_2+H <=> CH+H_2$	2.4E+17	-1.35	0
33.	${}^3CH_2+O => CO+H+H$	5.0E+13	0	0
34.	${}^3CH_2+O => CO+H_2$	3.0E+13	0	0
35.	${}^3CH_2+OH => CH_2O+H$	3.0E+13	0	0
36.	${}^3CH_2+OH <=> CH+H_2O$	1.1E+07	2.00	3000
37.	${}^3CH_2+O_2 => CH_2O+O$	5.0E+13	0	9000
38.	${}^3CH_2+O_2 => CO_2+H_2$	2.3E+12	0	600
39.	${}^1CH_2+M <=> {}^3CH_2+M$	3.6E+12	0	0
Third Body Efficiencies: N_2/1.7/ CO/9/ CO_2/6/ H/55/ H_2O/18/				
40.	${}^1CH_2+O_2 => CO+OH+H$	3.1E+13	0	0
41.	${}^1CH_2+CO_2 => CH_2O+CO$	6.6E+12	0	0

42.	$CH+H \iff C+H_2$	1.1E+14	0	0
43.	$CH+O \implies CO+H$	6.0E+13	0	0
44.	$CH+OH \implies HCO+H$	3.0E+13	0	0
45.	$CH+OH \iff C+H_2O$	4.0E+07	2.00	3000
46.	$CH+O_2 \implies HCO+O$	3.3E+13	0	0
47.	$CH+H_2O \implies CH_2O+H$	1.3E+15	-0.75	0
48.	$CH+CO_2 \implies HCO+CO$	3.4E+12	0	686
49.	$C+OH \implies CO+H$	5.0E+13	0	0
50.	$C+O_2 \implies CO+O$	6.0E+13	0	650
51.	$NH+H \iff N+H_2$	3.0E+13	0	0
52.	$NH+O \iff NO+H$	5.5E+13	0	0
53.	$NH+O \iff N+OH$	7.0E+11	0.50	0
54.	$NH+NO \iff N_2O+H$	1.2E+14	-0.30	0
55.	$N+OH \iff NO+H$	3.8E13	0	0
56.	$N+O_2 \iff NO+O$	6.4E+09	1.00	6280
57.	$N+NO \iff N_2+O$	3.3E+12	0.30	0
58.	$N_2O+M \iff N_2+O+M$	7.0E+14	0	56350
Third Body Efficiencies: $H_2O/5/$ $O_2/1.5/$ $N_2/1.5/$				
59.	$N_2O+H \implies N_2+OH$	7.6E+13	0	15200
60.	$HCN+O \implies NCO+H$	1.4E+04	2.64	4980
61.	$HCN+O \implies NH+CO$	3.5E+03	2.64	4980
62.	$HCN+OH \iff CN+H_2O$	1.5E+15	-0.68	12380
63.	$HCN+OH \implies NCO+H_2$	5.5E+03	2.67	10800
64.	$CN+OH \implies NCO+H$	6.0E+13	0	0
65.	$CN+O_2 \implies NCO+O$	1.0E+13	0	0
66.	$NCO+H \implies CO+NH$	5.0E+13	0	0
67.	$NCO+OH \implies NO+CO+H$	1.0E+13	0	0

16

68.	$NCO+NO \Rightarrow N_2O+CO$	3.0E+17	-1.53	260
69.	$CH+N_2 \Rightarrow HCN+N$	4.4E+12	0	22000
70.	$C+N_2 \Rightarrow CN+N$	6.3E+13	0	46000
71.	$^3CH_2+NO \Rightarrow HCN+OH$	2.3E+12	0	-1100
72.	$^1CH_2+NO \Rightarrow HCN+OH$	1.0E+14	0	0
73.	$CH+NO \Rightarrow HCN+O$	1.1E+14	0	0
74.	$C+NO \Rightarrow CN+O$	1.9E+13	0	0
75.	$C+NO \Rightarrow CO+N$	2.9E13	0	0
76.	$N+CO_2 \Rightarrow NO+CO$	1.3E+12	0	4950
77.	$N+CH_3 \Rightarrow HCN+2H$	7.1E+13	0	0
78.	$NH_3+H \Leftrightarrow NH_2+H_2$	6.36E+05	2.39	10171
79.	$NH_3+OH = NH_2+H_2O$	2.04E+06	2.04	566
80.	$NH_3+O \Leftrightarrow NH_2+OH$	2.10E+13	0	9000
81.	$NH_2+H \Leftrightarrow NH+H_2$	6.92E+13	0	3650
82.	$NH_2+OH \Leftrightarrow NH+H_2O$	4.00E+06	2	1000
83.	$NH_2+O \Leftrightarrow NH+OH$	6.75E+12	0	0
84.	$NH_2+O \Leftrightarrow HNO+H$	6.63E+14	-0.50	0
85.	$NH_2+NO \Leftrightarrow N_2+H_2O$	6.20E+15	-1.25	0
86.	$NH+OH \Leftrightarrow N+H_2O$	5.00E+11	0.50	2000.000
87.	$NH+OH \Leftrightarrow HNO+H$	2.00E+13	0	0
88.	$NH+O_2 \Leftrightarrow NO+OH$	7.60E+10	0	1530
89.	$NNH+OH \Leftrightarrow N_2+H_2O$	5.00E+13	0	0
90.	$NNH+NH_2 \Leftrightarrow N_2+NH_3$	5.00E+13	0	0
91.	$NNH+NO \Leftrightarrow N_2+HNO$	5.00E+13	0.000	0.000
92.	$NH_2+NO \Leftrightarrow NNH+OH$	6.40E+15	-1.250	0.000
93.	$HNO+M \Leftrightarrow H+NO+M$	1.50E+16	0	48680

Third Body Efficiencies: $H_2O/10/$ $O_2/2/$ $N_2/2/$ $H_2/2/$

17

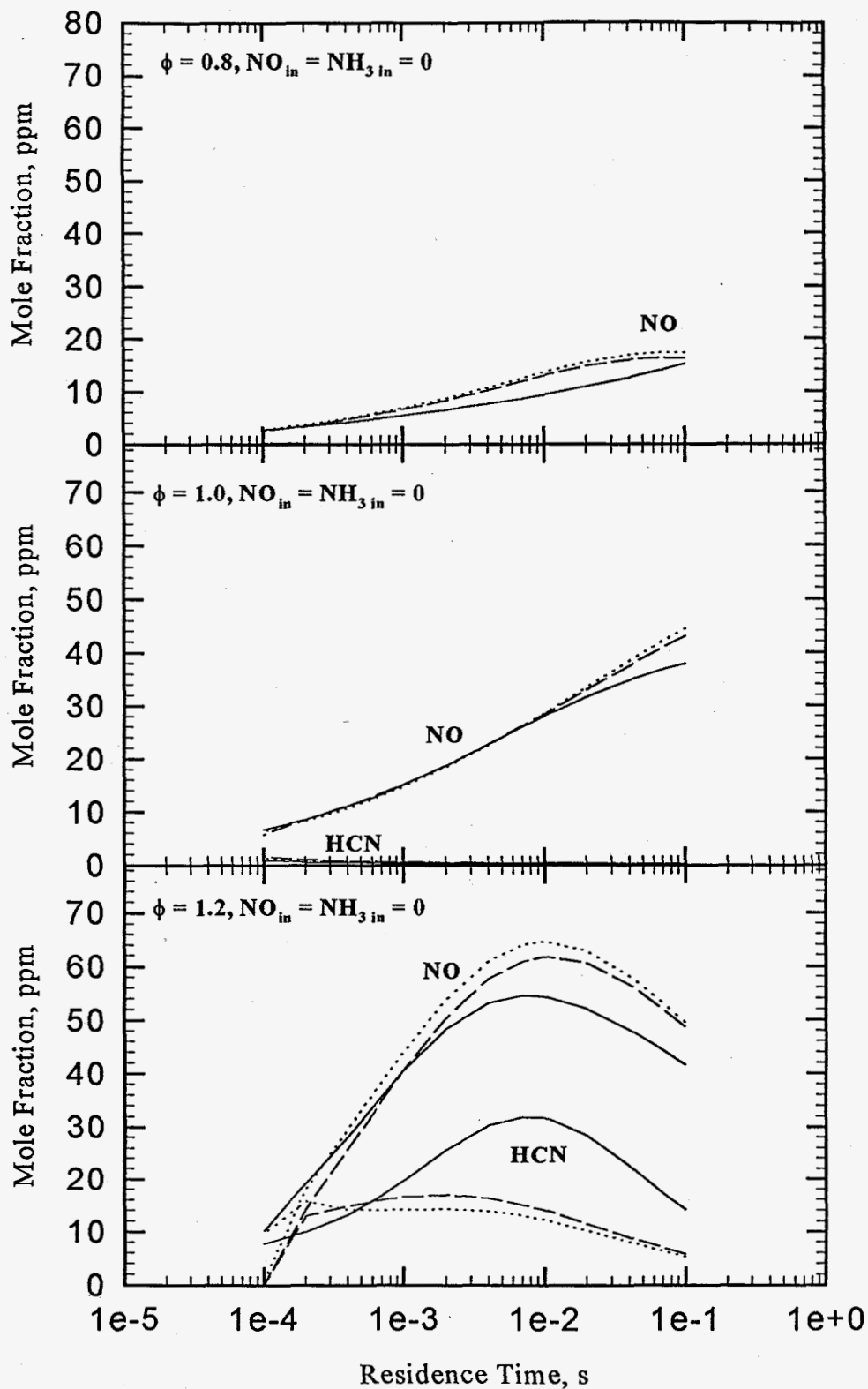| 94.	HNO+H<=>H_2+NO	5.00E+12	0	0
95.	HNO+OH<=>NO+H_2O	3.60E+13	0	0
96.	HNO+NH_2<=>NH_3+NO	2.00E+13	0.000	1000.000
97.	NH+O_2<=>HNO+O	1.00E+13	0.000	12000.000

Figure 1: Methane-air combustion in a perfectly-stirred reactor at a constant temperature of 1700 K: solid lines, detailed mechanism of Miller and Bowman; dashed lines, skeletal mechanism; dotted lines, reduced mechanism.
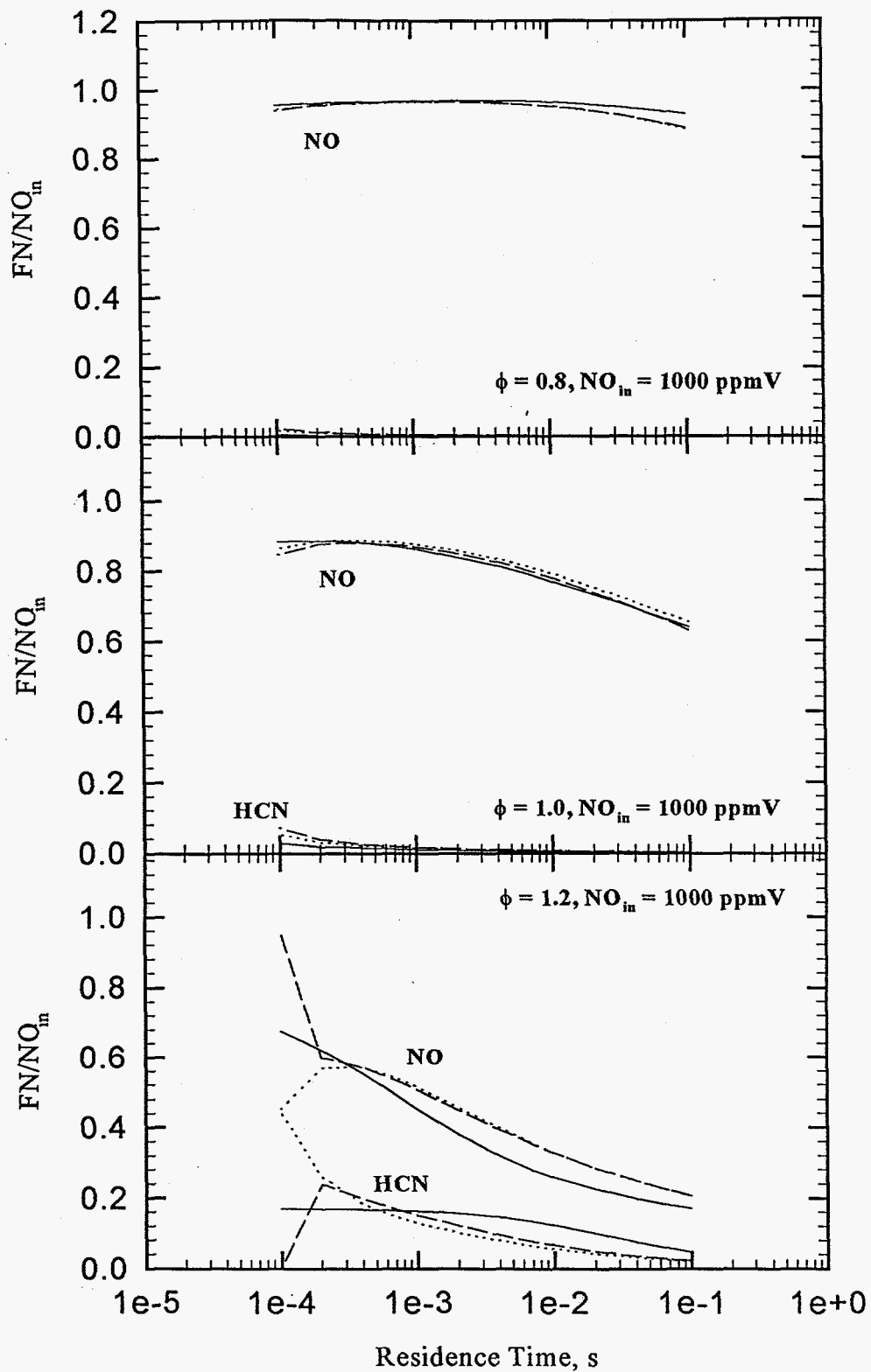
Figure 2: Methane-air combustion in a perfectly-stirred reactor at a constant temperature of 1700 K. Line symbols are the same as above. Molar ratios are plotted, where FN indicates the corresponding species.
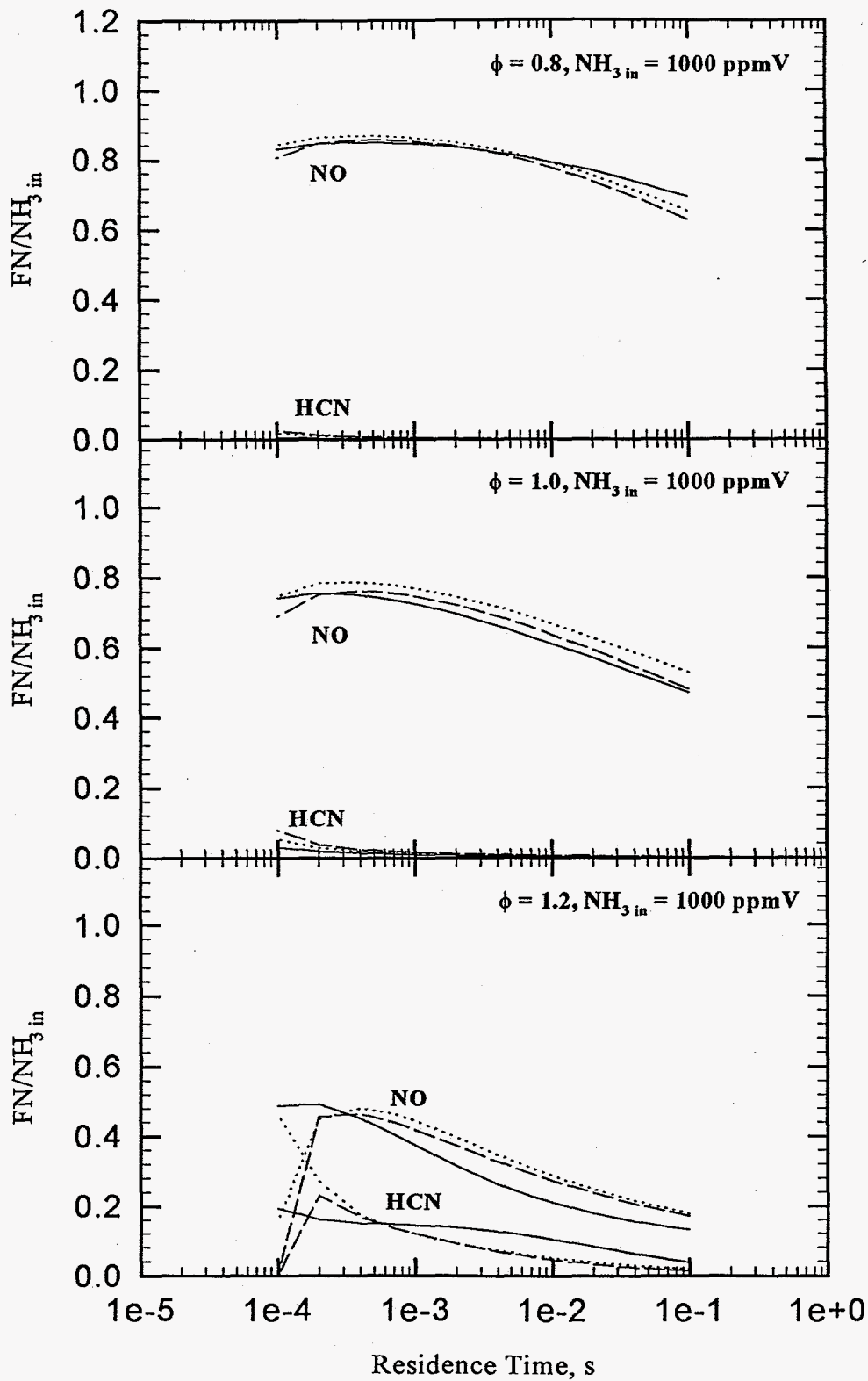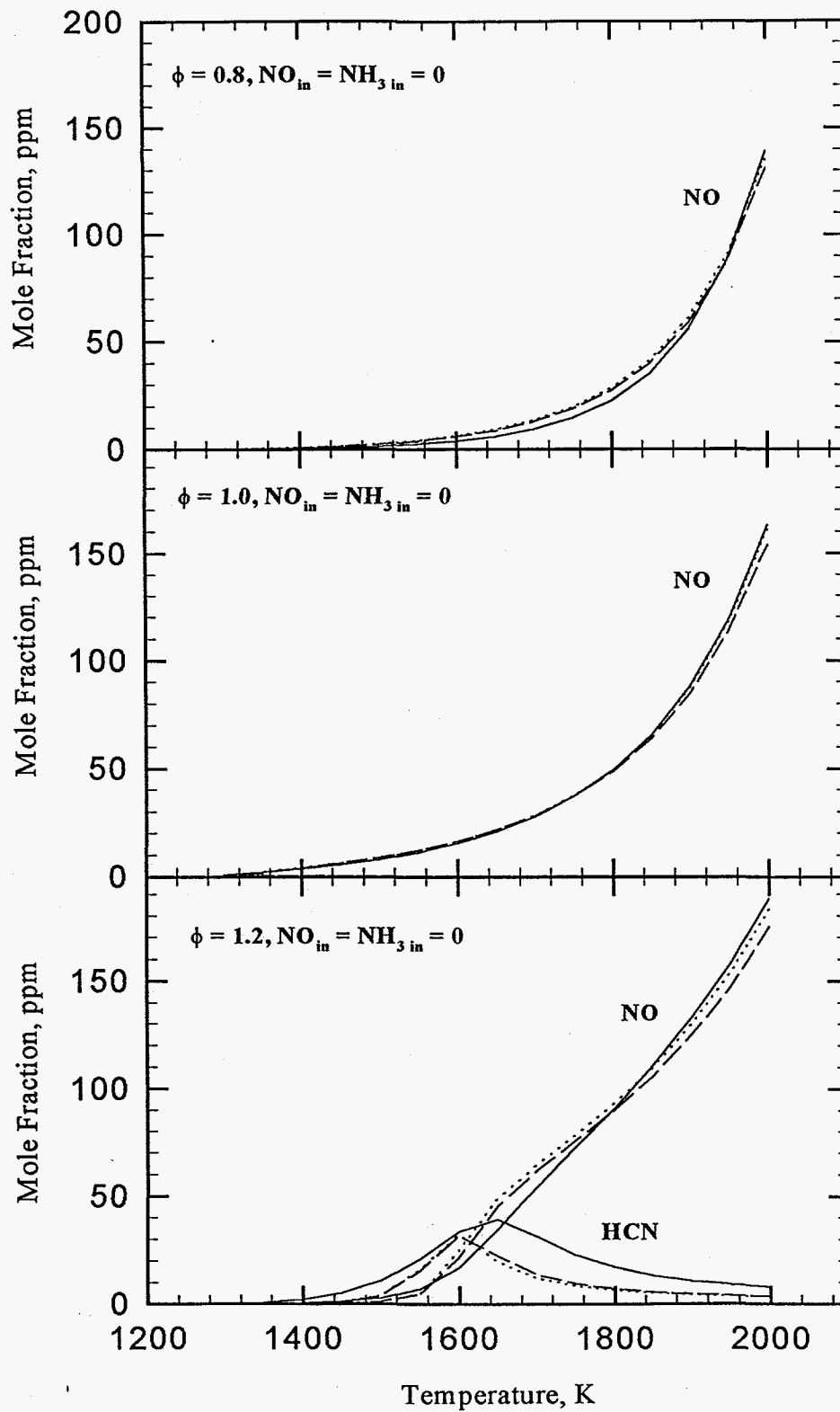
Figure 3: Methane-air combustion in a perfectly-stirred reactor at a constant temperature of 1700 K. Line symbols are the same as above. Molar ratios are plotted, where FN indicates the corresponding species.

Figure 4: Methane-air combustion at a constant residence time of 10^{-2} s: solid lines, detailed mechanism of Miller and Bowman; dashed lines, skeletal mechanism; dotted lines, reduced mechanism.
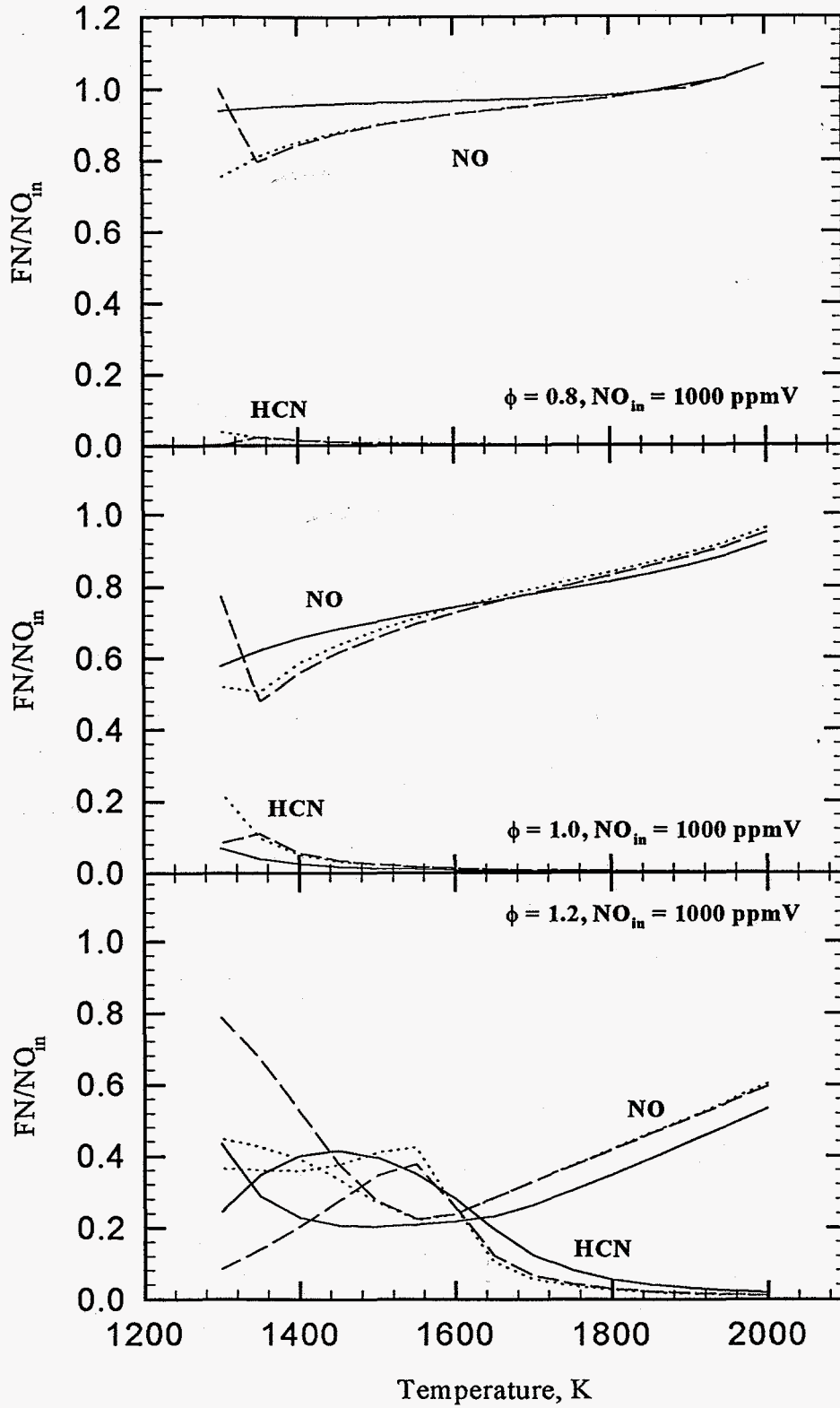
Figure 5: Methane-air combustion at a constant residence time of 10^{-2} s. Line symbols are the same as above. Molar ratios are plotted, where FN indicates the corresponding species.
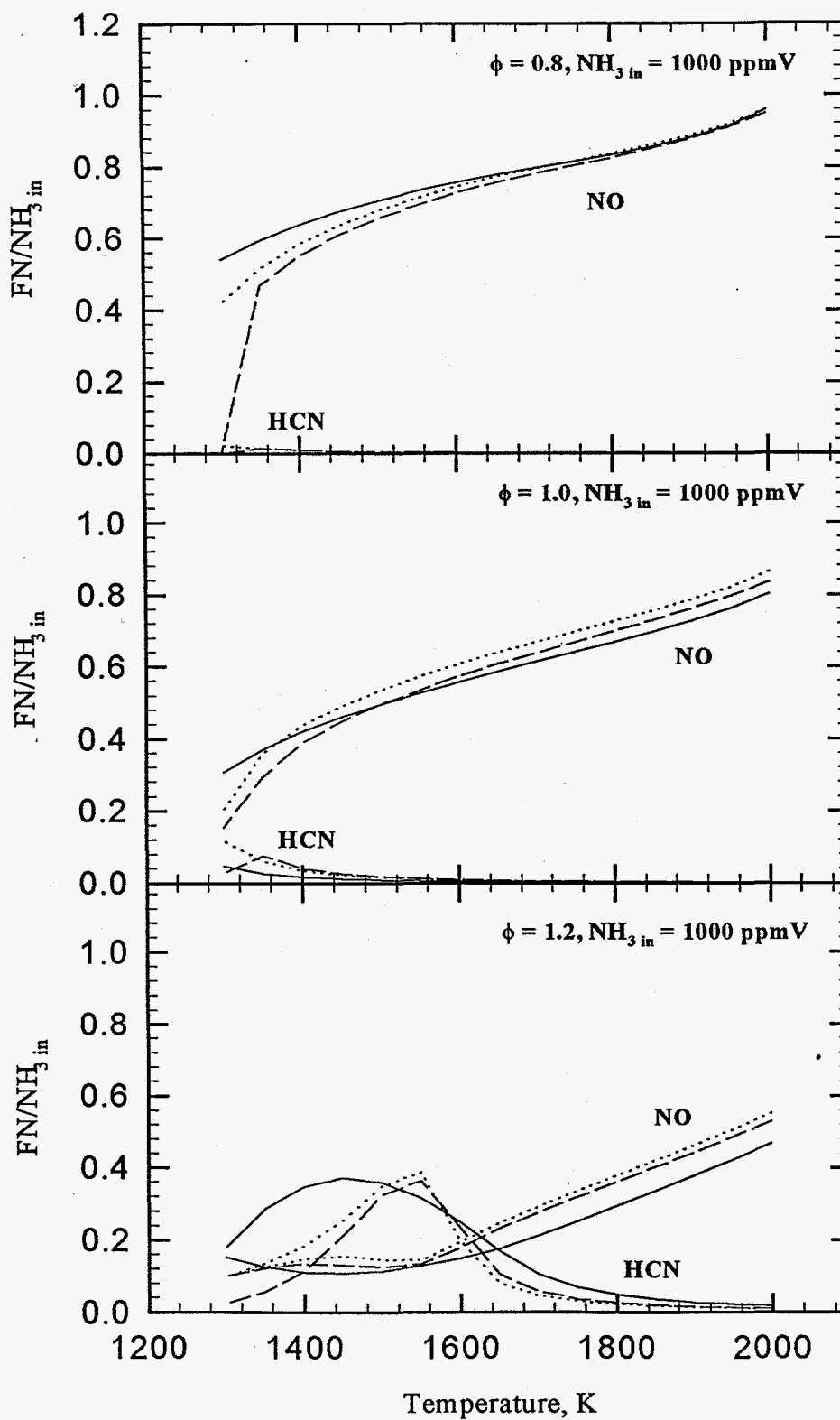
D. Marlow and T. S. Norton

Figure 6: Methane-air combustion at a constant residence time of 10^{-2} s. Line symbols are the same as above. Molar ratios are plotted, where FN indicates the corresponding species.